Multi-omics reveals Dengzhan Shengmai formulation ameliorates cognitive impairments in D-galactose-induced aging mouse model by regulating CXCL12/CXCR4 and gut microbiota

Jing-Yi Hou[1,2,3], He Xu[4], Guang-Zhao Cao[4], Liang-Liang Tian[4], Li-Han Wang[1,2,3], Nai-Qiang Zhu[3], Jing-Jing Zhang[4]* and Hong-Jun Yang[1,2]*

[1]Beijing Key Laboratory of Traditional Chinese Medicine Basic Research on Prevention and Treatment for Major Diseases, Experimental Research Center, China Academy of Chinese Medical Sciences, Beijing, China, [2]Robot Intelligent Laboratory of Traditional Chinese Medicine, Experimental Research Center, China Academy of Chinese Medical Sciences and MEGAROBO, Beijing, China, [3]Postdoctoral Mobile Research Station of China Academy of Chinese Medicine Sciences, Beijing, China, [4]Institute of Chinese Materia Medica, China Academy of Chinese Medical Sciences, Beijing, China

Dengzhan Shengmai (DZSM), a traditional Chinese medicine formulation, has been administered extensively to elderly individuals with cognitive impairment (CI). However, the underlying mechanisms by which Dengzhan Shengmai improves cognitive impairment remains unknown. This study aimed to elucidate the underlying mechanism of the effect of Dengzhan Shengmai on aging-associated cognitive impairment *via* a comprehensive combination of transcriptomics and microbiota assessment. Dengzhan Shengmai was orally administered to a D-galactose-induced aging mouse model, and evaluation with an open field task (OFT), Morris water maze (MWM), and histopathological staining was performed. Transcriptomics and 16S rDNA sequencing were applied to elucidate the mechanism of Dengzhan Shengmai in alleviating cognitive deficits, and enzyme-linked immunosorbent assay (ELISA), quantitative real-time polymerase chain reaction (PCR), and immunofluorescence were employed to verify the results. The results first confirmed the therapeutic effects of Dengzhan Shengmai against cognitive defects; specifically, Dengzhan Shengmai improved learning and impairment, suppressed neuro loss, and increased Nissl body morphology repair. Comprehensive integrated transcriptomics and microbiota analysis indicated that chemokine CXC motif receptor 4 (CXCR4) and its ligand CXC chemokine ligand 12 (CXCL12) were targets for improving cognitive impairments with Dengzhan Shengmai and also indirectly suppressed the intestinal flora composition. Furthermore, *in vivo* results confirmed that Dengzhan Shengmai suppressed the expression of CXC motif receptor 4, CXC chemokine ligand 12, and inflammatory cytokines. This suggested that Dengzhan Shengmai inhibited CXC chemokine ligand 12/CXC motif receptor

4 expression and modulated intestinal microbiome composition by influencing inflammatory factors. Thus, Dengzhan Shengmai improves aging-related cognitive impairment effects *via* decreased CXC chemokine ligand 12/CXC motif receptor 4 and inflammatory factor modulation to improve gut microbiota composition.

Highlights

- DZSM could improve cognitive impairments in elderly individuals.
- Multi-omics indicated that CXCR4 and its ligand (CXCL12) are the targets for improving cognitive impairment effects by DZSM, and also indirectly modulated the intestinal flora composition (*Bacteroidia*, *Erysipelotrichia*, and *Deferribacteres*).
- *In vivo*, enzyme-linked immunosorbent assay, quantitative real-time PCR, and immunofluorescence further confirmed that DZSM suppressed expression of CXCR4, CXCL12, and inflammatory cytokines (IL-18, IL-1β, IL-6, and TNF-α).
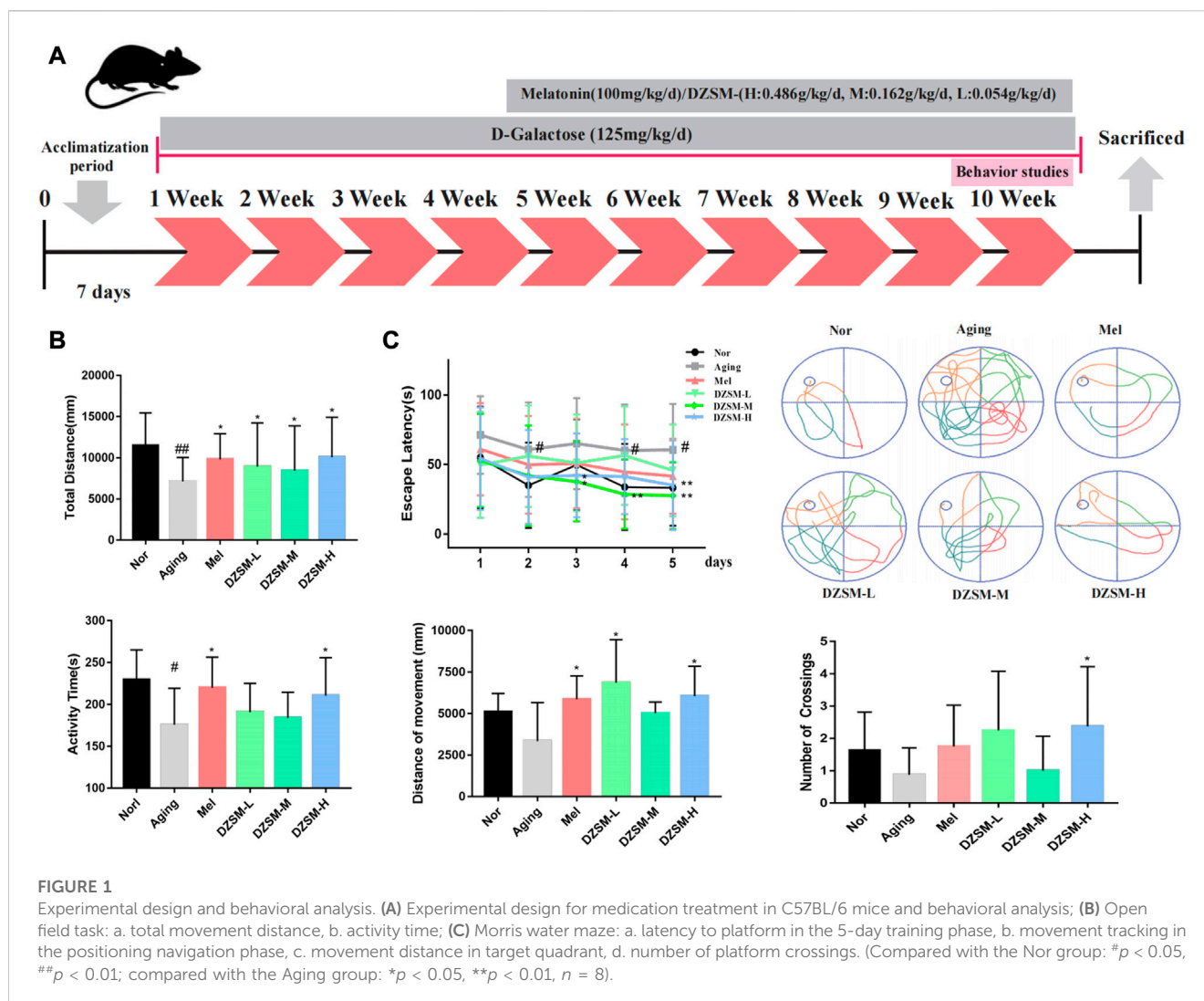
Introduction

Aging is naturally driven, regulated by multiple hormonal signaling pathways, and influenced by the interactions of various genetic and environmental factors (Estebsari et al., 2020). According to the World Population Prospects report, the percentage of the aging population of the world is expected to reach 16% by 2050 with improvements in the healthcare system, living conditions, and social welfare (Li et al., 2022). With global aging, the incidence of cognitive impairment (CI) continues to increase each year. CI refers to the gradual loss of cognitive ability and learning and memory ability (Eshkoor et al., 2015), seriously affecting quality of life and causing a heavy burden on families and society (Pei et al., 2020). Currently, the number of drugs for the treatment of age-related CI is very limited. These drugs include cholinesterase inhibitors (Battle et al., 2021) and excitatory amino acid receptor antagonists (Wang and Huang, 2018), but they have not been included in the standardized clinical treatment plans, as they have failed to show clinical treatment benefits (O'Brien et al., 2017). Therefore, the development of new therapies and drugs for improving CI and promoting the recovery of cognitive function in elderly adults still faces considerable challenges.

Dengzhan Shengmai (DZSM), a formulation derived from "Shengmai San," primarily contains four traditional Chinese medicine (TCM) ingredients, namely, the medicinal part of *Erigeron breviscapus* (Vaniot) Hand.-Mazz. (rhizoma), the medicinal part of *Panax ginseng* C.A. Mey., (rhizoma), the medicinal part of *Ophiopogon japonicas* (Thunb.) Ker-Gawl. (tubers), and the medicinal part of *Schisandra chinensis* (Turcz.) Baill., (dried fruit), in a weight ratio of 5:1:1:1.8 (drug approval number in Chinese Food and Drug Administration: Z20026439) (Mu et al., 2019). Among these TCM ingredients, *P. ginseng* C.A. Mey., and *S. chinensis* (Turcz.) Baill., the noted adaptogenic herbs (Slanina et al., 1997; Ratan et al., 2021), have been utilized as official

medicine in Russia, as well as recorded in Chinese Pharmacopoeia (2020 edition) (Chinese Pharmacopoeia Commission, 2020), Russian Federation's State Pharmacopoeia (14th edition) (The State Pharmacopoeia of Russian Federation, 2018), European Pharmacopoeia (10 edition) (European Pharmacopoeia, 2019), Japanese Pharmacopoeia (18 edition) (Society of Japanese Pharmacopoeia, 2021), and American herbal pharmacopoeia (2021 edition) (American herbal pharmacopoeia, 2021), and are known to have the following effects: nourishing blood, promoting blood circulation, invigorating vital energy, and nourishing *Qi*. *Ophiopogon* (Thunb.) Ker-Gawl., nourishes *Yin*, and is known to promote circulation and cleanse the heart. *S. chinensis* (Turcz.) Baill., functions as an astringent and nourishes *Qi*. *E. breviscapus* (Vaniot) Hand.-Mazz., promotes blood circulation and dredges collaterals. DZSM has been used clinically to improve cognitive dysfunction and forgetfulness for many years, and its efficacy and safety have also been reported in many clinical and experimental studies. Song et al., found that long-term use of DZSM could improve the score of Mini-mental State Examination (MMSE), Montreal Cognitive Assessment (MoCA), and Barthel Index, suggesting that DZSM effectively improves CIs and cognitive dysfunctions (Song et al., 2018). A meta-analysis of randomized clinical trials also indicated that DZSM appears to alleviate neurological function impairment and improves quality of life in elderly individuals. In addition, Sheng et al. (2017) and Zhang et al. (2020) demonstrated that DZSM and its active components effectively protect against cognitive deficits of Alzheimer's Disease (AD) and improve aging-related learning and memory deficits by accelerating the aggregation of Aβ, reducing Aβ-oligomer formation, and mediating changes in white matter microstructure functions. As the underlying mechanism of multi-ingredient and multi-pharmacological formulations to improve aging-related neurocognitive impairment has not yet been fully elucidated, further research is needed.

Owing to the rise of "omics" technologies, the underlying mechanisms of TCM in the treatment of complex and chronic diseases have been systematically elucidated in multiple dimensions and levels (Hou et al., 2022). Among these "omics" technologies, transcriptomics is based on the study of overall gene transcription and transcriptional regulation (Hou et al., 2021), while the study of intestinal flora is based on the distribution and composition of gut microbiotas (Lin et al., 2021). The systematic integration of multi-omics provides a systematic mechanistic understanding of multi-component formulas targeting complex diseases through multi-targeting (Yang et al., 2022). In this study, we investigated the role of DZSM against aging-associated CIs by further exploring how DZSM ameliorates CI in a D-galactose-induced aging mouse model based on the comprehensive integration of transcriptomics and gut microbiota, attempting to provide a scientific basis for transcriptomic microbiome-based intervention in CI.

FIGURE 1
Experimental design and behavioral analysis. **(A)** Experimental design for medication treatment in C57BL/6 mice and behavioral analysis; **(B)** Open field task: a. total movement distance, b. activity time; **(C)** Morris water maze: a. latency to platform in the 5-day training phase, b. movement tracking in the positioning navigation phase, c. movement distance in target quadrant, d. number of platform crossings. (Compared with the Nor group: $^{#}p < 0.05$, $^{##}p < 0.01$; compared with the Aging group: $^{*}p < 0.05$, $^{**}p < 0.01$, $n = 8$).

Materials and methods

Chemicals and reagents

DZSM formulation dry powder voucher specimens were provided by Yunnan Bio Valley (China, No: 20190023). D-galactose (purity, ≥99%) and melatonin (purity, ≥99%) were purchased from Sigma-Aldrich (St. Louis, United States). A CXC chemokine ligand 12 (CXCL12)-targeting antibody and the chemokine CXC motif receptor 4 (CXCR4)-targeting antibody were purchased from Proteintech Group Co., Ltd., (Chicago, IL). DNase/RNase free water, phosphate-buffered saline (PBS) and Bovine Serum Albumin (BSA) were purchased from Solarbio (Beijing, China). A FastPure RNA Extraction Kit and SYBR qPCR Master Mix were purchased from Vazyme Biotech Co., Ltd., (Nanjing, China). An M5 Super Plus qPCR RT kit was purchased from Mei5 Biotechnology Co., Ltd., (Beijing, China). Enzyme-linked immunosorbent assay (ELISA) kits for CXCL12, CXCR4, interleukin-1β (IL-1β), interleukin-6 (IL-6), interleukin-18 (IL-18), and tumor necrosis factor-α (TNF-α) were purchased from Elabscience Biotechnology Co., Ltd., (Wuhan, China).

UPLC/MS for chemical fingerprints

The DZSM formulation dry powder was accurately weighted (0.50 g) and ultrasonically extracted with 40 mL of 50% methanol for 60 min; the supernatant was then filtrated before analysis, using a 0.45 μm filter. A HPLC system coupled with an Orbitrap mass spectrometer (Agilent, United States) was applied for the LC-MS analysis, and a Leapsil (C18, 2.7 μm, 150 mm × 2.1 mm) was used for all analyses. The mobile phase comprised of 0.1% formic acid-water (A) and 0.1% formic acid-acetonitrile (B). These were used for the gradient elution program as follows: 0%–15% B (0–1 min); 15%–30% B (1–29 min); 30%–32% B (29–31 min); 32%–38% B (31–37 min); 38%–43% B (37–48 min); 43%–55% B (48–54 min); 55%–70% B (54–70 min); 70%–90% B (70–76 min); and 90% B (76–86 min). We loaded 2 μL of the samples with a flow rate of 300 μL/min for the mobile phase. In the positive/negative polarity mode, electrospray ionization (ESI) source was employed with a

TABLE 1 Results of UPLC-MS/MS analysis of DZSM.

NO.	RT time (min)	Molecular weight	Formula	Mode	Ingredients
1	6.68/4.393	382.08	$C_{17}H_{18}O_{10}$	Positive/Negative	4-CDOA
2	8.33	288.06	$C_{15}H_{12}O_6$	Positive	Eriodictyol
3	10.85/17.65	516.12	$C_{25}H_{24}O_{12}$	Positive/Negative	4,5-diCQA
4	12.94/13.60	544.12	$C_{26}H_{24}O_{13}$	Positive/Negative	Erigoster B
5	13.35	448.10	$C_{21}H_{20}O_{11}$	Positive	Narigenin-7-glucuronide
6	13.96/14.36	446.08	$C_{21}H_{18}O_{11}$	Positive/Negative	Breviscapine
7	16.75/10.60	286.04	$C_{15}H_{10}O_6$	Positive/Negative	Luteolin
8	18.49/36.43	638.44	$C_{36}H_{62}O_9$	Positive/Negative	Ginsenoside f1
9	33.12/33.55	800.49	$C_{42}H_{72}O_{14}$	Positive/Negative	Ginsenoside Rg1
10	36.43/50.064	766.48	$C_{42}H_{70}O_{12}$	Positive/Negative	Ginsenoside Rk1
11	37.34/54.13	620.42	$C_{36}H_{60}O_8$	Positive/Negative	Ginsenoside Rh4
12	38.01	400.18	$C_{23}H_{28}O_6$	Positive	Schisandrin
13	45.63	432.21	$C_{24}H_{32}O_7$	Positive	Schisandol A
14	51.07	416.18	$C_{23}H_{28}O_7$	Positive	gomisin o
15	54.31	514.22	$C_{28}H_{34}O_9$	Positive	gomisin f
16	66.92	416.21	$C_{24}H_{32}O_6$	Positive	Schisandrin A
17	3.83	354.09	$C_{16}H_{18}O_9$	Negative	Narigenin-7-glucuronide
18	7.04	448.09	$C_{21}H_{20}O_{11}$	Negative	Narigenin-7-glucuronide
19	24.95	558.13	$C_{27}H_{26}O_{13}$	Negative	acetyl-di-CQA
20	38.06	1078.59	$C_{53}H_{90}O_{22}$	Negative	Notoginsenoside L
21	41.79	946.54	$C_{48}H_{82}O_{18}$	Negative	Ginsenoside Re

scanning model of Spray Voltage (kV) at 3.6 and 3.3 kV, respectively. Full MS/dd-MS^2 at full scan (m/z 100–1,700) was performed while maintaining the capillary temperature at 350°C. Subsequently, Compound Discoverer 3.2 was utilized for retention time correction and peak extraction, and mzCloud online database (https://www.mzcloud.org/) was employed for substance identification based on secondary spectrum information.

Animal grouping and medication treatment

Male C57BL/6J mice (age, 16 weeks; weight, 25–28 g) were purchased from Beijing Jinmuyang Biotechnology Co., Ltd., (Beijing, China; certification No. SCXK (Jing) 2019-0010). All experimental procedures were performed in accordance with the rules of care and the use of basic theories of Chinese Medical Sciences (Approval No. 2022B029). All animals were kept at 25.0oC ± 1.0°C with a 12-h light-dark cycle and free access to food and water. As a neuroendocrine hormone, melatonin exhibits a wide range of physiological activities, including reducing oxidative stress, immune modulation, neuroprotection, improving CI, and improving learning and memory (Dai et al., 2021). Therefore, we selected melatonin as the positive drug to control in the current study. After 7 days of

adaptation, the mice were randomly divided into six groups ($n = 10$): normal (Nor), aging (Aging), melatonin (Mel), and DZSM (DZSM-L, DZSM-M, and DZSM-H) groups. As shown in Figure 1A, the CI model was established by intraperitoneal injection of D-galactose (125 mg/kg/d) for 10 weeks. Mice in the Mel and DZSM groups (DZSM-L, DZSM-M, and DZSM-H) received oral melatonin (100 mM/kg) or DZSM (0.054 g/kg/d, 0.162 g/kg/d, 0.486 g/kg/d), respectively, for 6 weeks, after 4 weeks of D-galactose induction. Behavioral testing was carried out during the 10th week, after which, all mice were euthanized humanely, and their brain tissues were collected.

Behavioral observations

Open field task (OFT)

An OFT was used to evaluate the locomotor activity of the mice. Briefly, the mice were independently placed within an empty area (30 cm × 30 cm) and permitted to move freely for 3 min to obtain the data.

Morris water maze (MWM)

A MWM experiment was performed to detect escape latency and spatial positioning. The experimental procedure was carried out
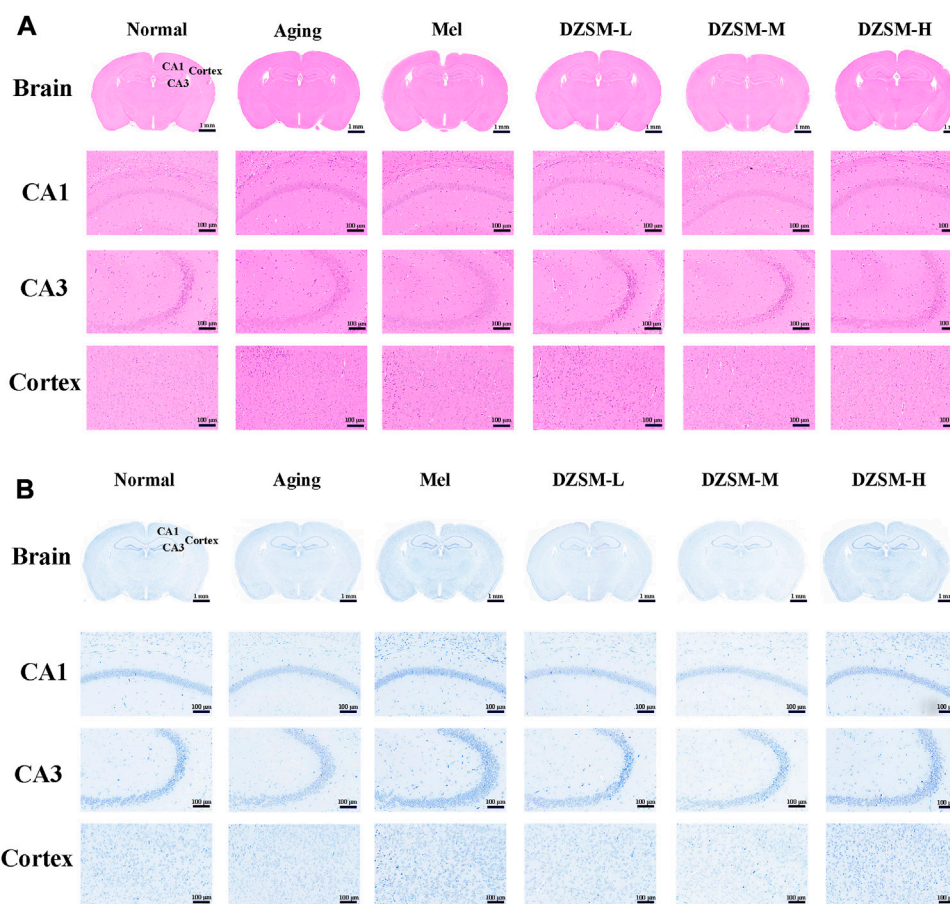
FIGURE 2
Histopathological changes in the brain tissue. **(A)** H&E staining; **(B)** Nissl staining (n = 3). Bar length: 1 mm, 100 µm.

for 7 days. On the first day, the mice were placed in the pool to adapt to the environment. Each mouse was randomly left to find the platform within 1 min on days 2–5. If the mice reached the platform within the allotted time, they were allowed to rest at the platform for 15 s; mice failing to reach the platform within 1 min were directed to the platform and allowed to rest for 15 s. On day 6, the platform was hidden below the surface, and the escape time of each mouse was tested for 60 s. On the last day, after the removing the platform, we recorded the frequency with which each mouse crossed the location where the platform had previously been located.

Histopathological staining

The harvested brain tissues were fixed with 4% paraformaldehyde for 24 h, and the fixed brain slices were dehydrated and embedded to prepare paraffin sections. The paraffin samples were cut into 5-µm sections for staining with hematoxylin and eosin (H&E) and Nissl, after which, the histopathological changes of the brain tissues could be examined.

Transcriptomics analysis using high-throughput sequencing

Total RNA was extracted from the brain tissues of mice in the Nor, CI, and DZSM-H groups (n = 3) using TRIzol Reagent. Applied Protein Technology (Shanghai, China) constructed the cDNA libraries using RNA, and they were sequenced on an Illumina Novaseq 6000/MGISEQ-T7 instrument according to a standardized sequencing protocol. Differentially expressed genes (DEGs) between groups were analyzed using the "limma" package and determined according to the conditions as follows: |log2(Fold Change)| > 0.58 and p-value < 0.05. Gene Ontology (GO) and Kyoto Encyclopedia of Genes and Genomes (KEGG) enrichment of DEGs at both Aging-vs.-Nor and DZSM-H-vs.-Aging groups were implemented by the DAVID database (https://david.ncifcrf.gov/) and Metascape (https://metascape.org/gp/index.html#/main/step1). The protein-protein network (PPI) of reversed DEGs was constructed by STRING database (https://cn.string-db.org/), and visualized in Cytoscape 3.7.2 platform. The topological parameter of nodes and interaction edges in the network was calculated by cytoHubba plug-in, and the nodes with top degrees were considered as key targets.

16S rRNA high-throughput sequencing for gut microbiota

Ten mice were randomly selected from the Nor, CI, and DZSM-H groups, and 0.1 g of fresh feces was collected. Microbial DNA was first extracted using the HiPure Soil DNA Kits. Following the extraction of microbial DNA, the V3+V4 region of 16S rDNA was amplified with specific barcoded primers. The PCR product was quantified by the ABI StepOnePlus Real-Time PCR System (Life Technologies, United States). The samples were sequenced on an Illumina platform by Genedenovo Biotechnology Co., Ltd., (Guangzhou, China). After sequencing the raw reads, UPARSE was applied to cluster tag (>97%) identities into operational taxonomic units (OTUs); the number of OTUs were then computed. The composition of microbiota, α-diversity, and β-diversity analyses were performed. Thereafter, linear discriminant analysis (LDA) effect size (LEfSe), with a threshold size of >2, was applied to compare differences in the taxa between the Aging-vs.-Nor and DZSM-vs.-Aging groups. Redundancy analysis (RDA) and Spearman analysis were employed to identify the correlations between key targets/inflammatory factors and microorganisms.

Enzyme-linked immunosorbent assay (ELISA)

Harvested brain tissues ($n = 8–10$) were homogenized in PBS with a glass homogenizer on ice, and the protein concentrations were quantified using a BCA Protein Assay Kit. The levels of CXCL12, CXCR4, IL-1β, IL-6, IL-18, and TNF-α in the brain tissue were determined using the ELISA kits, according to the following procedures: the samples were added to the wells and immobilized with specific antibodies for 90 min; they were incubated with biotinylated detection Ab working solution for 60 min; and the wells were triple washed with washing buffer. Corresponding horseradish peroxidase (HRP) conjugate working solution was then added for another 30 min of incubation, followed by 5-fold washing with a washing buffer before measurements.

Quantitative real-time PCR

The FastPure RNA Extraction Kit was applied to the extracted total RNA from brain tissues ($n = 3$), which reverse-transcribed to cDNA using the M5 Super Plus qPCR RT kit. The SYBR qPCR Master Mix was then applied to detect mRNA expression. Primers for the detected genes are listed in Supplementary Table S1. The relative expression of mRNA was calculated as $2^{-\Delta\Delta CT}$.

Immunofluorescence (IF) staining

Briefly, the brain tissue sections ($n = 3$) were permeabilized with Triton X-100, followed by 5% BSA for sealing, and incubated with anti-CXCR4 (1:150 with 2% BSA) and anti-CXCL12 (1:100 with 2% BSA) antibodies overnight at 4°C. On the following day, the corresponding secondary antibodies (diluted 1:200) were incubated on the sections with DAPI (1:1000). Finally, images of the sections were captured under a fluorescence microscope.

Statistical analysis

Statistical analyses were performed using GraphPad Prism 7.0 software, and all data analyses were conducted with one-way variance analysis (ANOVA) and the Tukey post-hoc test. A p-value of <0.05 was considered significant.

Results

Identification of chemical components of DZSM

As shown in Table 1, a preliminary analysis revealed 21 ingredients detected by UPLC-MS/MS, including 4-CDOA, Eriodictyol, 4,5-diCQA, Erigoster B, Narigenin-7-glucuronide, Breviscapine, Luteolin, Ginsenoside f1, Ginsenoside Rg1, Ginsenoside Rk1, Ginsenoside Rh4, Schisandrin, Schisandol A, gomisin o, gomisin f, Schisandrin A, 4-CQA, Narigenin-7-glucuronide, acetyl-di-CQA, Notoginsenoside L, and Ginsenoside Re. The total ion chromatogram (TIC) is shown in Supplementary Figure S1.

DZSM attenuated cognitive deficits and pathological changes

The OFT and MWM tests were performed at week 10 to assess changes in autonomous behavior, exploration and learning, and memory abilities. As shown in Figure 1B, compared with those in the Nor group, the total distance and activity time were significantly reduced in the Aging group. Compared with those of the Aging group, the movement distance was significantly larger in all medication groups, activity times were somewhat increased in the DZSM-L and DZSM-M groups, and activity times were significantly increased in the DZSM-H and Mel groups. In Figure 1C, the MWM results showed that in the positioning and navigation experiment, compared with that of the Nor group, the initiation period of the Aging group was significantly prolonged; the initiation periods of all medication groups were significantly shorter, especially those of the DZSM-M group on days 3–5, which were significantly reduced. In the space exploration experiment, compared with measurements in the Nor group, the movement distances of the Aging group decreased in the target quadrant, and the number of platform crossings decreased. In contrast, the movement distances within the target quadrant and the number of platform crossings in the medication groups increased significantly. Movement distances in the target quadrant were significantly increased in the Mel, DZSM-L, and DZSM-H groups, and the number of platform crossings was significantly increased in the DZSM-H group. These results provide evidence that DZSM was beneficial for improved learning and memory ability and recovery of cognitive performance in D-galactose-induced aging mice.
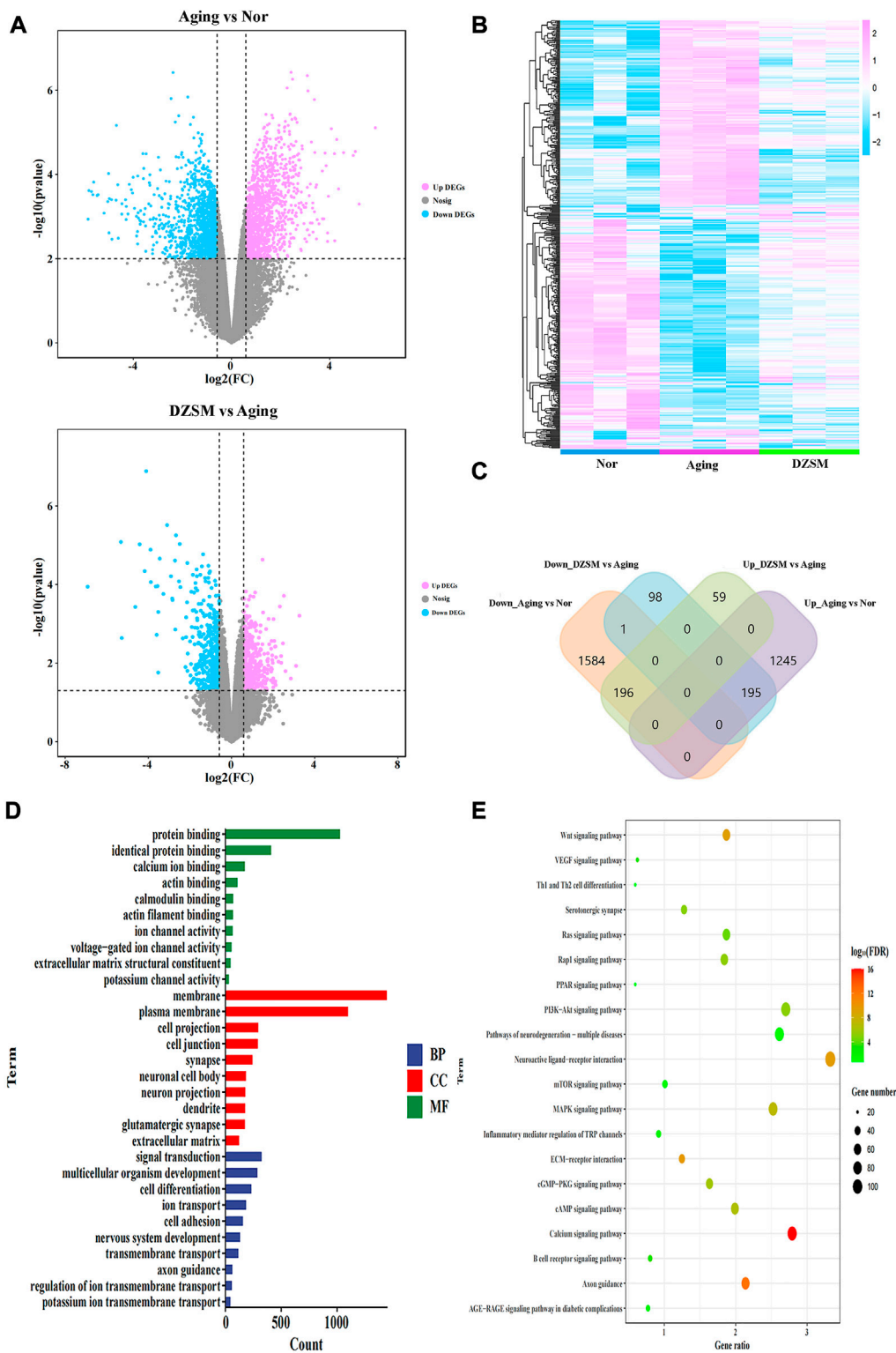
FIGURE 3
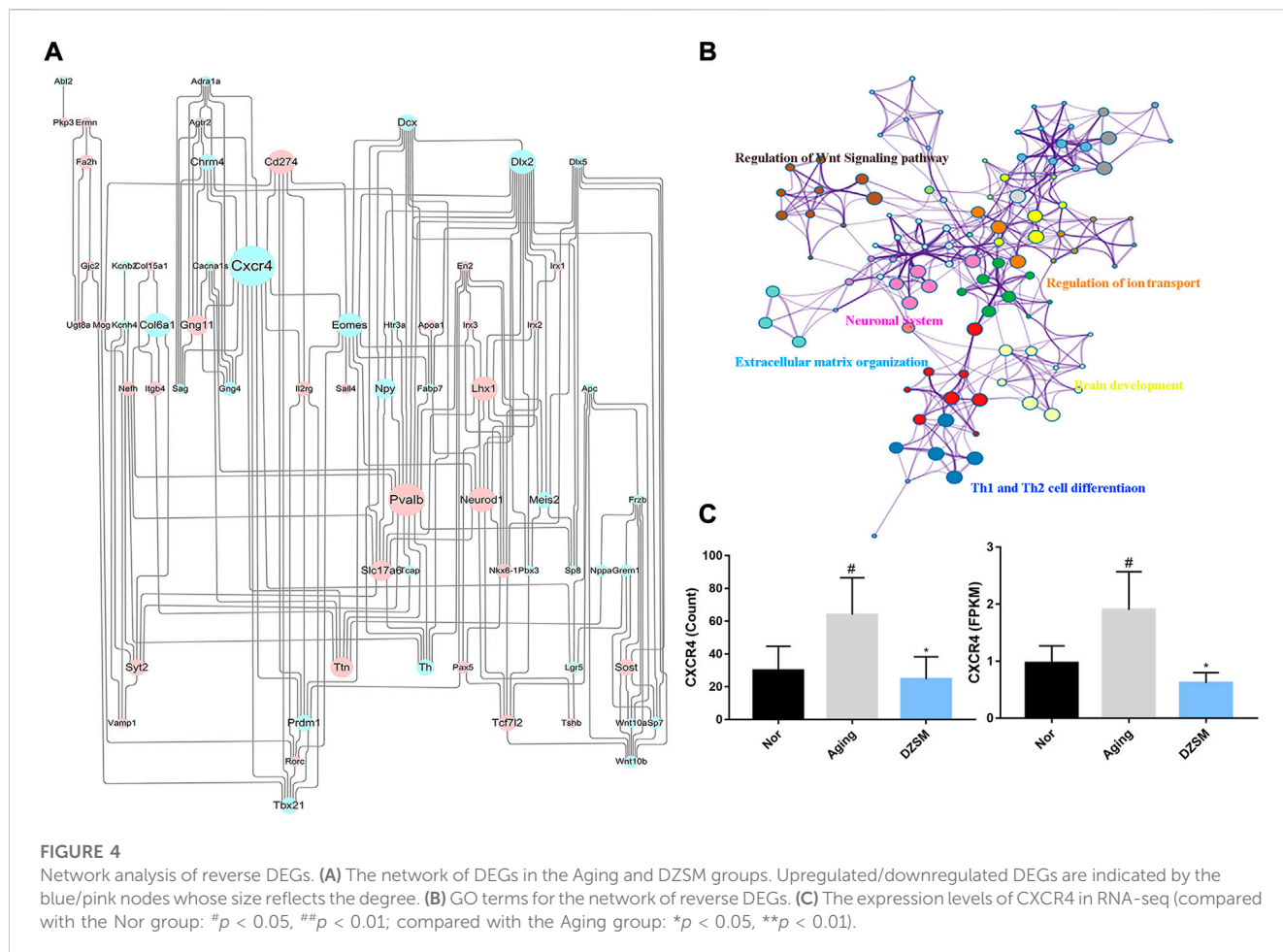Transcriptomics analysis. **(A)** Volcano map of the DEGs in the Aging vs. Normal (Nor) groups and the DZSM vs. Aging groups; **(B)** Heatmap of the DEGs in the Nor, Aging, and DZSM groups; **(C)** Venn diagram of the DEGs in the Nor, Aging, and DZSM groups; **(D)** GO enrichment analysis of DEGs (red terms represent MF, green terms represent CC, and blue terms represent BP). **(E)** KEGG pathway analysis of DEGs.

FIGURE 4
Network analysis of reverse DEGs. **(A)** The network of DEGs in the Aging and DZSM groups. Upregulated/downregulated DEGs are indicated by the blue/pink nodes whose size reflects the degree. **(B)** GO terms for the network of reverse DEGs. **(C)** The expression levels of CXCR4 in RNA-seq (compared with the Nor group: $^\#p < 0.05$, $^{\#\#}p < 0.01$; compared with the Aging group: $^*p < 0.05$, $^{**}p < 0.01$).

As shown in Figure 2A, H&E staining showed that compared with those in the Nor group, neurons in the Aging group were sparsely arranged, the number of irregularly shaped cells increased, and cell nuclei shrank. Significantly less neuron reduction was observed in mice treated with DZSM. In Figure 2B, on Nissl staining, no obvious pathological changes were discovered in cells of the Nor group, while the number of Nissl bodies was significantly reduced, and neuronal morphology was disrupted in the D-galactose-induced Aging group. The number of Nissl bodies was increased, and their morphologies were better in the Mel and DZSM groups (DZSM-L, DZSM-M, DZSM-H), suggesting that DZSM might effectively reduce D-galactose-induced brain tissue damage in aging mice.

Identification of targets for the amelioration of CI by DZSM using transcriptomics analysis

The DEGs were screened based on significant *p*-values < 0.05 and |log2(Fold Change)| > 0.58 (Figure 3A). Measured against the Nor group, 3220 DEGs were identified in the Aging group, with 1,440 of them upregulated and 1,780 downregulated. After DZSM treatment, 548 DEGs were identified, with 255 upregulated and 293 downregulated. As shown in Figures 3B, C, the results of hierarchical cluster analysis suggested that after DZSM administration, some gene expression induced by

D-galactose was reversed. Venn mapping was used to further clarify the DEG distribution after DZSM administration. These results suggested that D-galactose upregulated the expression of 1,440 DEGs. DZSM reversed the upregulation of 195 DEGs present in the Aging-vs.-Nor groups and downregulation of DEGs in the DZSM-vs.-Aging groups. By comparing the downregulated and upregulated genes in the Aging-vs.-Nor and DZSM-vs.-Aging groups, respectively, we also observed that the expression of 1,781 DEGs was downregulated after D-galactose treatment. The expression of 196 of these DEGs was reversed after DZSM administration, indicating that DZSM might ameliorate the aging effects induced by D-galactose. Enrichment analysis of the DEGs in the Aging-vs.-Nor groups and the DZSM-vs.-Aging groups was performed to elucidate the origins of DZSM amelioration of cognitive deficits in aging mice. As shown in Figure 3D, biological process (BP) analysis indicated that the enriched DEGs in the Aging-vs.-Nor groups and the DZSM-vs.-Aging groups were closely associated with signal transduction. The cellular component (CC) terms were mainly related to membrane and extracellular matrix, and the molecular function (MF) terms were related to the protein and identical protein binding. Furthermore, pathway analysis has suggested that the DEGs were enriched mainly in inflammation and signal transduction, such as the "Th1 and Th2 cell differentiation," "Wnt signaling," "Ras signaling," and "MAPK signaling" pathways (Figure 3E).
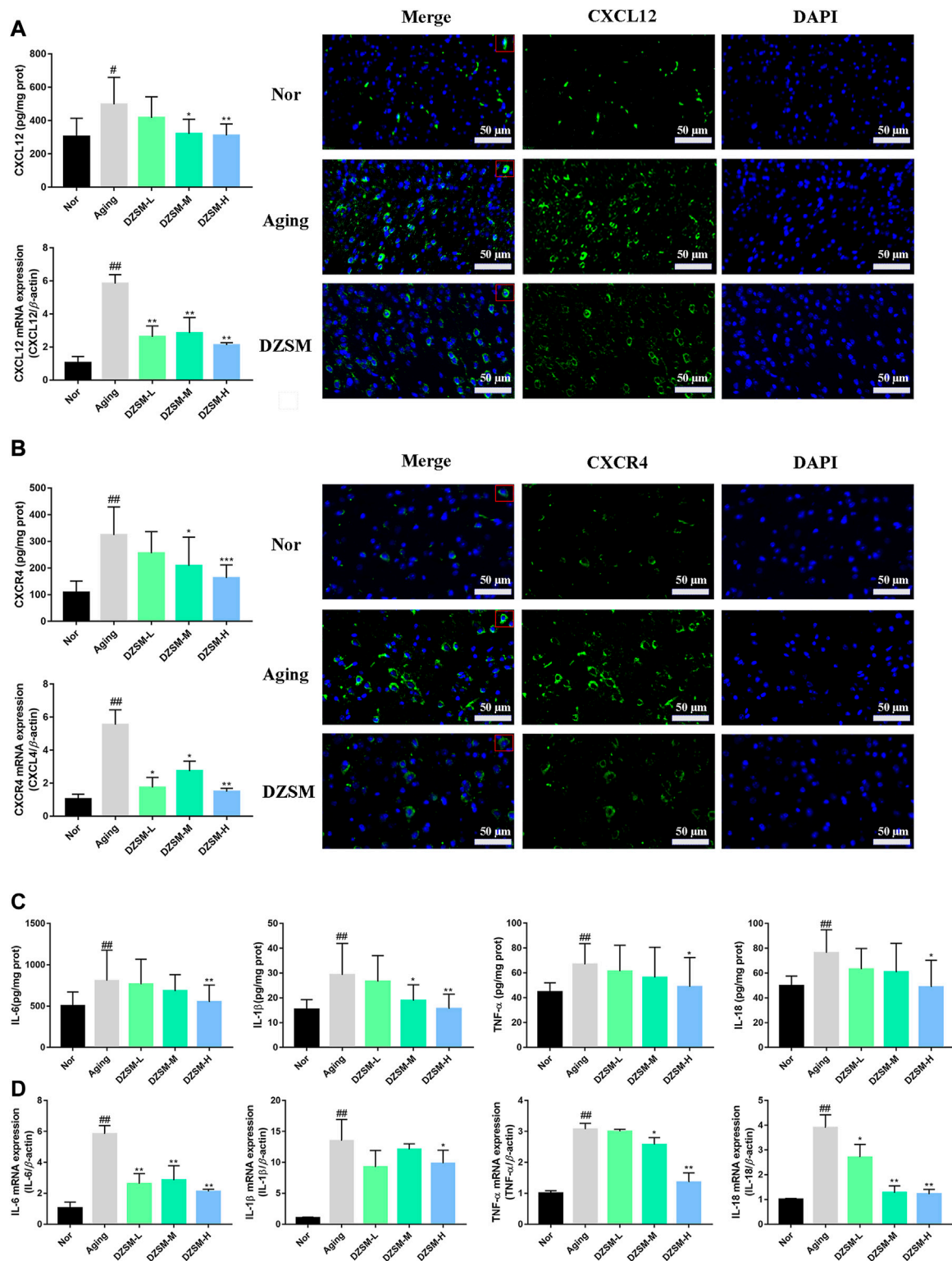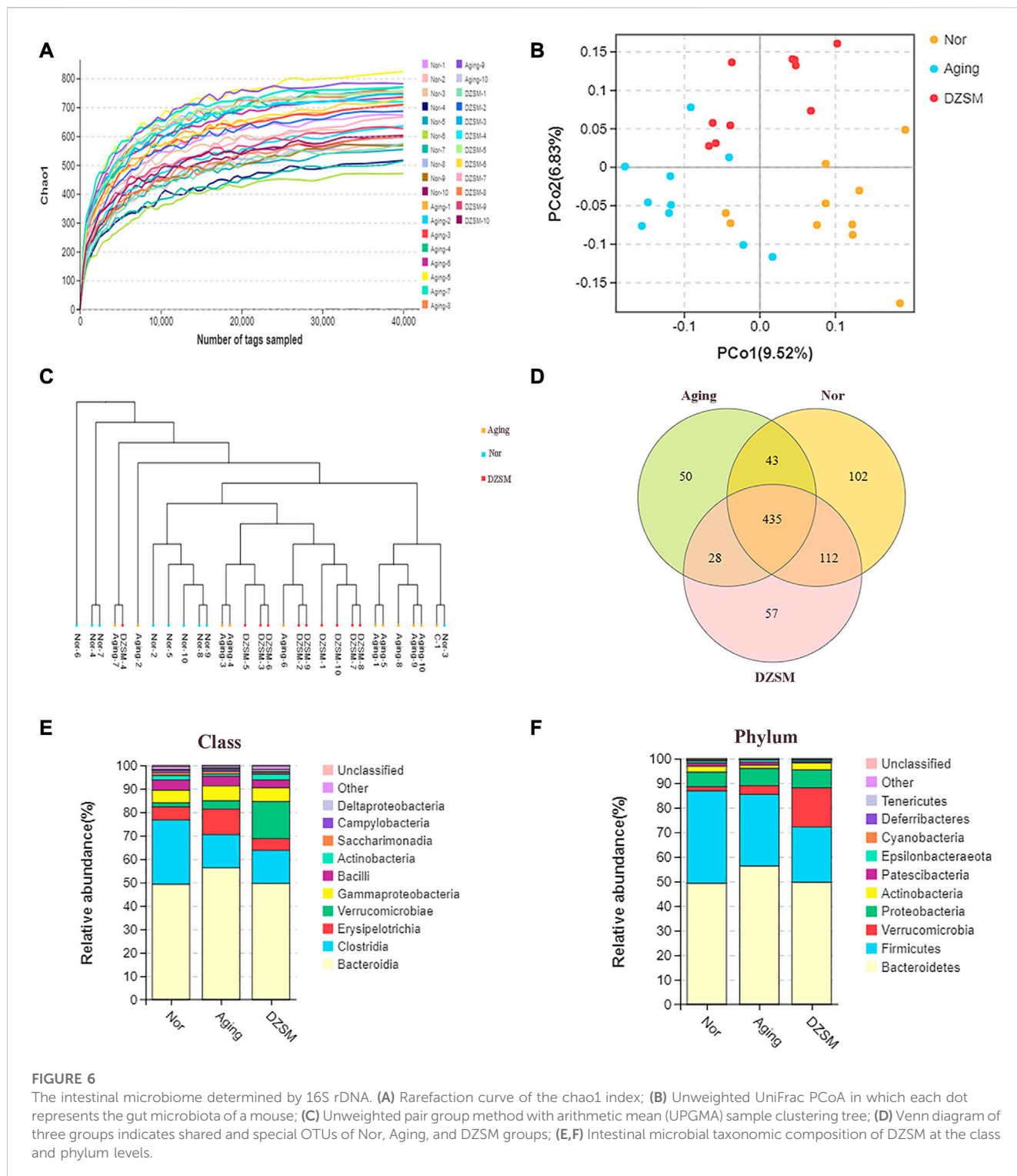
FIGURE 5
DZSM downregulated CXCR4 and CXCR12 expression and inhibited inflammatory cytokine production. **(A)** RT-PCR, ELISA, and IF analysis of CXCR4 (Bar length: 50 μm); **(B)** RT-PCR, ELISA, and IF analysis of CXCL12 (Bar length: 50 μm); **(C)** Analysis of IL-1β, IL-6, TNF-α, and IL-18 levels by ELISA. **(D)** RT-PCR analysis of IL-1β, IL-6, TNF-α, and IL-18 (compared with the Nor group: $^{#}p < 0.05$, $^{##}p < 0.01$; compared with the Aging group: $^{*}p < 0.05$, $^{**}p < 0.01$).

FIGURE 6
The intestinal microbiome determined by 16S rDNA. **(A)** Rarefaction curve of the chao1 index; **(B)** Unweighted UniFrac PCoA in which each dot represents the gut microbiota of a mouse; **(C)** Unweighted pair group method with arithmetic mean (UPGMA) sample clustering tree; **(D)** Venn diagram of three groups indicates shared and special OTUs of Nor, Aging, and DZSM groups; **(E,F)** Intestinal microbial taxonomic composition of DZSM at the class and phylum levels.

To further explore the potential mechanism of DZSM in attenuating cognitive deficits in aging mice, the identified upregulated/downregulated DEGs in the Aging-vs.-Nor groups and the DZSM-vs.-Aging groups were uploaded to the STRING online database (https://string-db.org/) (combined score of >0.7). A PPI network was then constructed, and the Cytoscape 3.7.2 platform was used to visualize the PPI network with 251 nodes and 506 interaction edges (Figure 4A). Based on the network's

topological properties calculated using the cytoHubba plug-in, CXCR4 (degree = 19) emerged as the principal target in the PPI network, indicating that it may be the key target affected by DZSM. Furthermore, the DEGs with reversed expression between the Aging-vs.-Nor and DZSM-vs.-Aging groups were enriched mainly in GO terms associated with inflammation and signal transduction, including "regulation of the Wnt signaling pathway," "regulation of ion transport," "Th1 and Th2 cell

differentiation," "neuronal system," "extracellular matrix organization," and "brain development" (Figure 4B). The results of RNA-seq also demonstrated that DZSM significantly reduced the expression levels of CXCR4 and CXCL12 in the Aging group at the FPKM and count levels (Figure 4C). Given these results, we preliminarily speculate that DZSM may regulate the processes of inflammation and signal transduction to ameliorate cognitive function in D-galactose–induced aging mice.

DZSM reduced expression of CXCL12/CXCR4 and inhibited expression of pro-inflammatory cytokines

CXCL12, also known as stromal cell-derived factor-1 (SDF-1), is the only known ligand of CXCR4, and increasing evidence has indicated that CXCL12/CXCR4 signal transduction participates in regulating neuroimmunology, inflammatory, and neurodegenerative related diseases (Isles et al., 2019; Sanfilippo et al., 2020). As shown in Figures 5A, B, D-galactose led to a sharply increased expression of CXCR4 and CXCL12 at both the protein and gene levels, and these levels were decreased after the DZSM intervention. Recent studies have demonstrated that major pro-inflammatory cytokines, including IL-6, IL-1β, IL-18, and TNF-α, appear to be more closely associated with cognitive dysfunction, and pronounced in elderly and post-operative individuals (Ricker et al., 2011; Hou et al., 2020). Numerous studies have further validated that CXCL12/CXCR4 signal transduction, where directed or undirected, can mediate neuroinflammatory cytokines during cognitive dysfunction, leading to the activation of glial cells and disturbance of immune homeostasis (Shi et al., 2016; Mai et al., 2021). Therefore, our investigation further evaluated the expression of pro-inflammatory cytokines both at the gene and protein levels, as shown in Figures 5C, D, and our results demonstrated that DZSM significantly suppressed the expression of IL-6, IL-1β, IL-18, and TNF-α, compared with that of the Aging group, suggesting that DZSM might work by balancing the immune response through moderating CXCL12/CXCR4 signal transduction and preventing disruption of steady immune homeostasis.

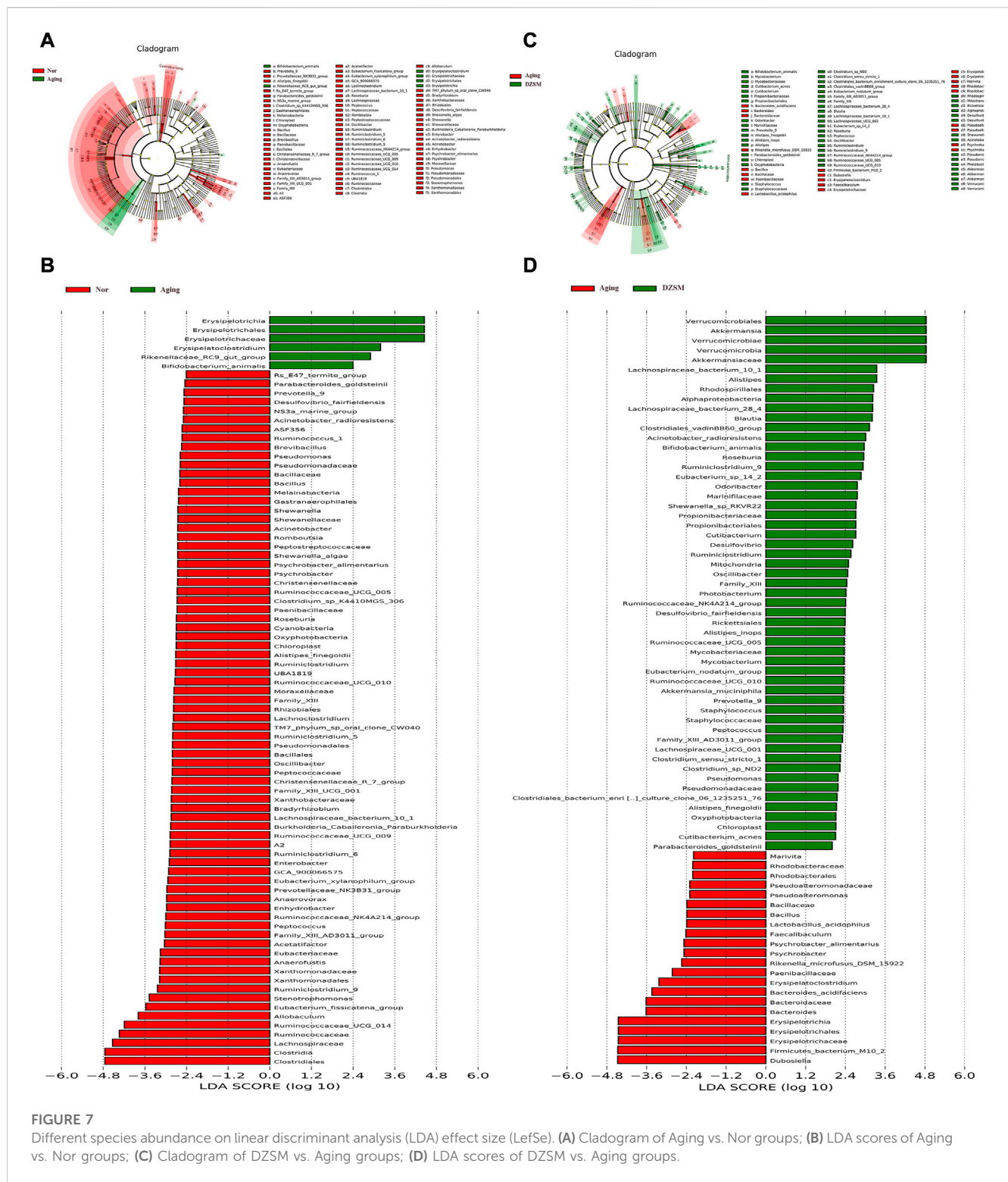## DZSM effects on intestinal flora

In this study, to investigate the effect of DZSM on mice after D-galactose-induced aging, 30 stool samples were collected, and bacterial 16S rDNA sequencing was performed. The analysis results in a total of 2,804,340 valid reads, which were filtered at a 97% identify threshold to yield 17,790 species-classification OTUs. The chao1 curve (Figure 6A) approached the saturation plateau and suggested that the vast majority of microorganisms were detected by 16S rRNA high-throughput sequencing. As shown in Figures 6B, C, the principal coordinate analysis (PCoA) and unweighted pair group method with arithmetic mean (UPGMA) clustering analysis demonstrated differentials between the Nor, Aging, and DZSM groups. Based on the Venn mapping of Nor vs. Aging vs. DZSM, the diversity of intestinal flora in the Aging group was reduced significantly by 19.12%, compared with the Nor group, and this was reversed in the DZSM intervention group (Figure 6D). As observed

in Figure 6E, Bacteroidia, Erysipelotrichia, Gammaproteobacteria, and Actinobacteria classes were represented with average loads of 49.18%, 5.54%, 5.41%, and 1.86%, respectively, in the Nor group. In the Aging group, the proportion of Actinobacteria reduced to 0.94%, and the proportion of Bacteroidia, Erysipelotrichia, and Gammaproteobacteria increased sharply to 56.27%, 10.84%, and 6.38%, respectively. In the DZSM group, the levels of Bacteroidia, Erysipelotrichia, and Gammaproteobacteria, reversed to 49.59%, 4.99%, and 5.89%, respectively, and Actinobacteria increased to 2.33%. At the phylum level, Bacteroidetes accounted for approximately 50%, and DZSM restored the proportion of Bacteroidetes induced by D-galactose (56.27%) back to 49.59%. There were also similar tendencies of reversal in the proportions of Actinobacteria, Cyanobacteria, and Deferribacteres, from 2.38%, 0.27%, and 0.19%, respectively, in the Nor group, to 1.32%, 0.18%, and 0.09%, respectively, in the Aging group, and to 2.78%, 0.24%, and 0.11%, respectively, in the DZSM group (Figure 6F).

To further investigate the alterations of DZSM in aging mice, LEfSe analysis was applied to identify and compare the key taxa contributing to the different microbiota compositions of the Nor, Aging, and DZSM-H groups. As shown in Figures 7A, B six biomarkers, including Erysipelotrichia, Erysipelotrichales, Erysipelotrichaceae, Erysipelatoclostridium, Rikenellaceae_RC9_gut_group, and Bifidobacterium_animalis, were enriched in the Aging group. Furthermore, 20 taxa (Prevotella_9, Alistipes_finegoldii, Parabacteroides_goldsteinii, Oxyphotobacteria, Chloroplast, Family_XIII, Family_XIII_AD3011_group, Lachnospiraceae_bacterium_10_1, Roseburia, Peptococcus, Oscillibacter, Ruminiclostridium, Ruminiclostridium_9, Ruminococcaceae_NK4A214_group, Ruminococcaceae_UCG_005, Ruminococcaceae_UCG_010, Desulfovibrio_fairfieldensis, Acinetobacter_radioresistens, Pseudomonadaceae, and Pseudomonas) were more abundant in the DZSM group and overlapped with the Nor group (Figures 7C, D).

DZSM regulated CXCL12/CXCR4 signal transduction and inhibited inflammatory cytokines, improving microbes according to integrated transcriptomics and intestinal microbiota analysis
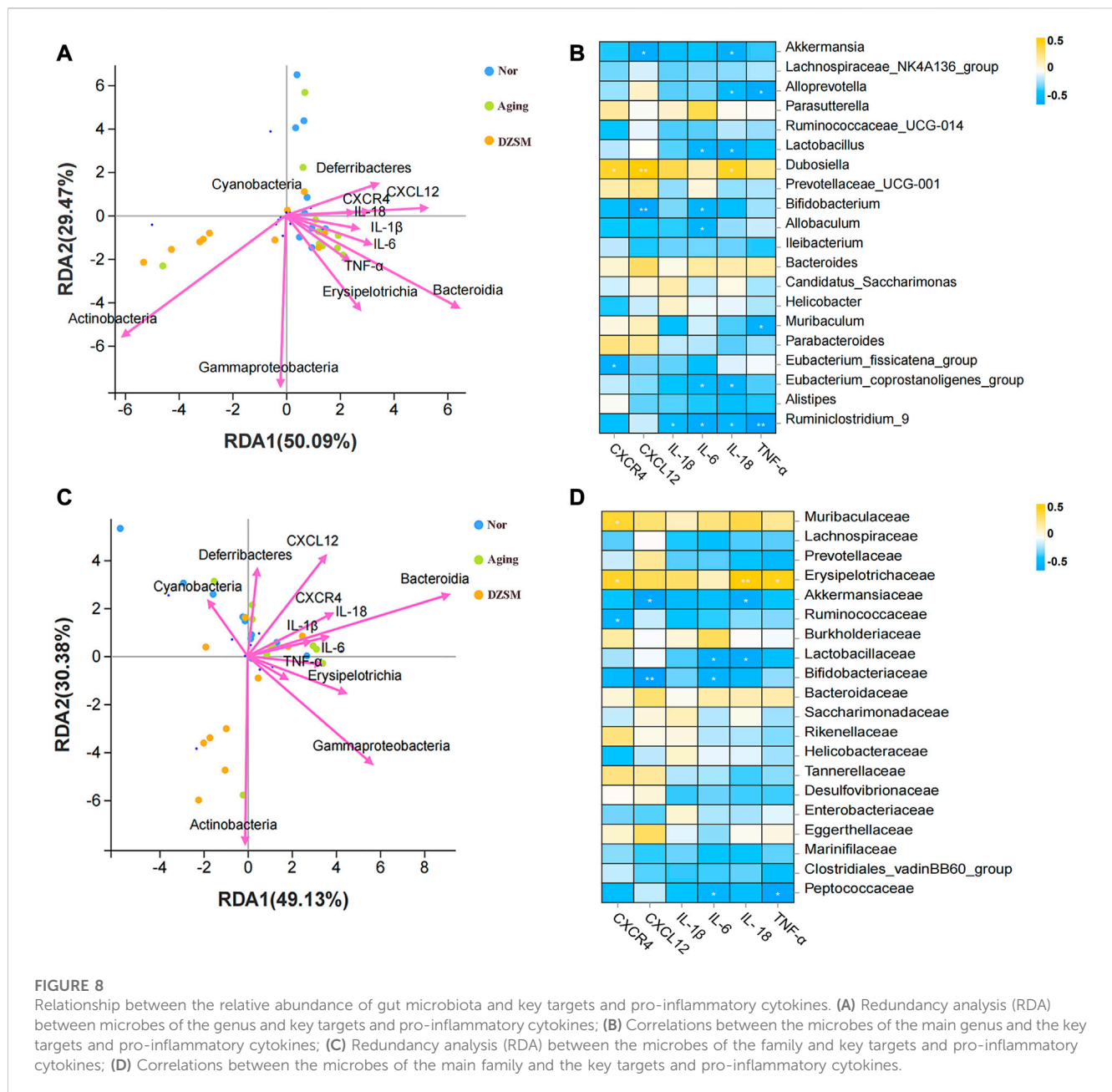
The relationship between the gut microbiota and the key targets/pro-inflammatory cytokines was investigated using RDA and Spearman correlation analyses. As Figures 8A, C demonstrate, Bacteroidia, Erysipelotrichia, and Deferribacteres showed close positive associations with CXCR4, CXCL12, and inflammatory factors IL-1β, IL-6, IL-18, and TNF-α, both at genus and family levels. Akkermansia, Bifidobacterium, and Ruminiclostridium_9 were negatively correlated with CXCR4 and CXCL12, as well as inflammatory factors IL-1β, IL-6, IL-18, and TNF-α at the genus level. Akkermansiaceae, Lactobacillaceae, Bifidobacteriaceae, and Peptococcaceae were also negatively associated with CXCR4, CXCL12, IL-1β, IL-6, IL-18, and TNF-α at the family level (Figures 8B, D). These results suggested that the DZSM exerted ameliorating CI effects in D-galactose-induced aging mice via regulation of the distribution and composition of the gut microbiota and the release of inflammatory factors.

FIGURE 7
Different species abundance on linear discriminant analysis (LDA) effect size (LefSe). **(A)** Cladogram of Aging vs. Nor groups; **(B)** LDA scores of Aging vs. Nor groups; **(C)** Cladogram of DZSM vs. Aging groups; **(D)** LDA scores of DZSM vs. Aging groups.

Discussion

The aging of the global population is a rapidly growing phenomenon, which not only triggers many age-related diseases but also imposes significant social and economic burdens on society. One of the well-known features of the aging process is the development of cognitive deficits and impairments in learning
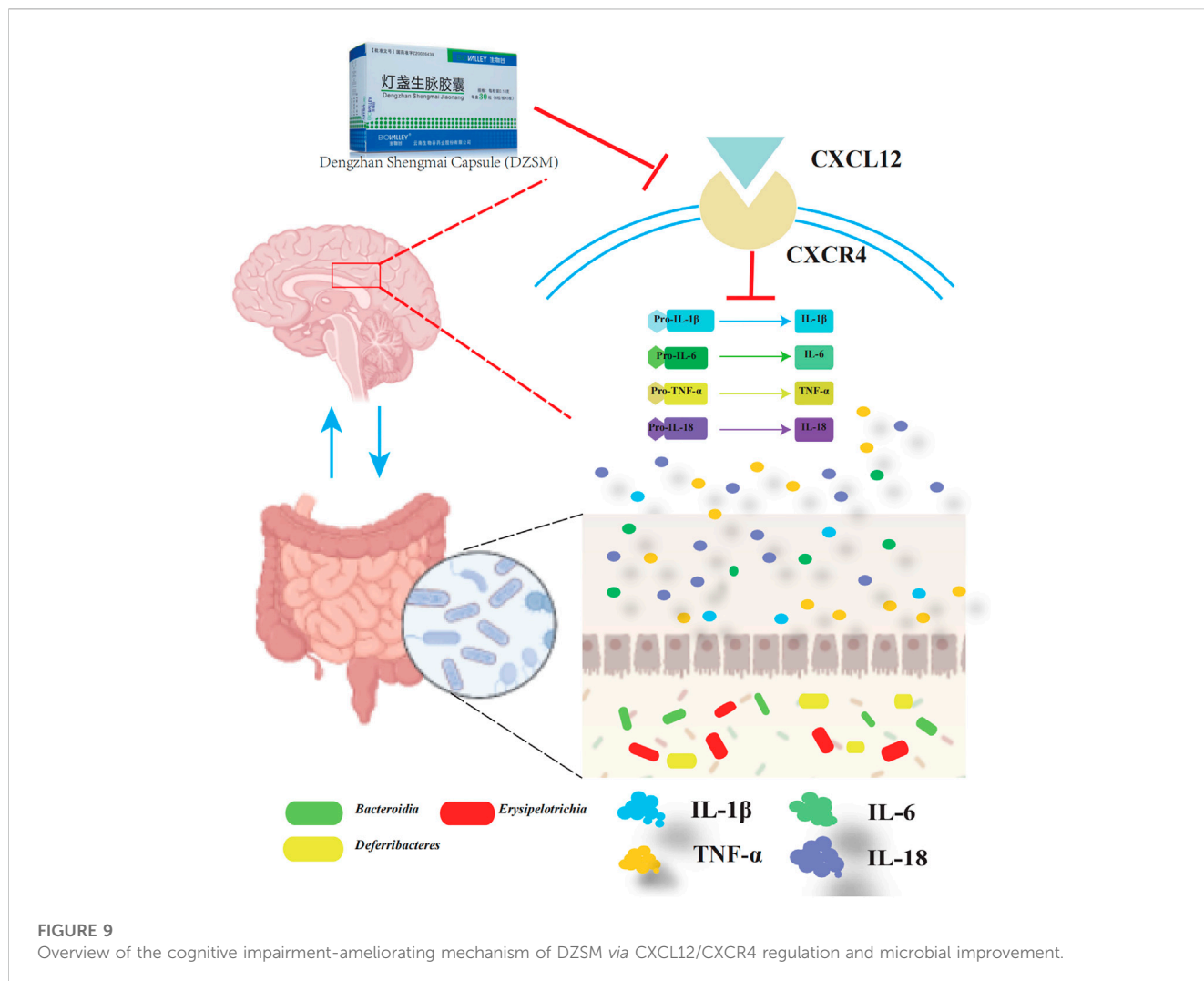
and memory (Go et al., 2018; Khan et al., 2019). The present study investigated the neuroprotective effects of DZSM, a traditional Chinese formulation, against CI in D-galactose-induced aging mice. Using an accelerating aging mouse model, DZSM (0.162 g/kg/d or 0.486 g/kg/d) treatment for 6 weeks was found to improve learning and memory abilities, reduce neural loss, and repair Nissl body morphology. Transcriptomics and gut

FIGURE 8
Relationship between the relative abundance of gut microbiota and key targets and pro-inflammatory cytokines. **(A)** Redundancy analysis (RDA) between microbes of the genus and key targets and pro-inflammatory cytokines; **(B)** Correlations between the microbes of the main genus and the key targets and pro-inflammatory cytokines; **(C)** Redundancy analysis (RDA) between the microbes of the family and key targets and pro-inflammatory cytokines; **(D)** Correlations between the microbes of the main family and the key targets and pro-inflammatory cytokines.

microbiota analysis suggested that DZSM's therapeutic effect may be mediated through CXCR4 by regulating inflammatory responses and signal transduction processes, while *Bacteroidia*, *Erysipelotrichia*, and *Deferribacteres* may be key in alleviating CIs. Additionally, DZSM was found to decrease the levels of CXCR4, CXCL12, and multiple pro-inflammatory cytokines, including TNF-α, IL-6, IL-1β, and IL-18 in aging mice, indicating its ability to mitigate neuroinflammation and exert a neuroprotective effect.

Chronic exposure to D-galactose (i.p.) is a reliable method for inducing aging and CI models, as it triggers multiple symptoms such as neuroinflammation, oxidative stress, neurodegeneration, and learning and memory impairments (Li et al., 2019). To replicate the complex pathological features of aging, we established an aging-like mouse model using D-galactose (i.p.) in this study. Our findings indicated that the D-galactose-induced mice exhibited significant cognitive dysfunction and pathological impairment, consistent with previous studies, including increased neuroinflammation, oxidative damage, and decreased exploration, learning, and memory abilities (Budni et al., 2016; Sun et al., 2018). Interestingly, DZSM, with its various anti-oxidative, anti-inflammatory, and neuroprotective agents such as scutellarin, caffeic acid, ginsenoside Rb3, ginsenoside Rg1, ginsenoside Re, and schisandrin, may function as a crucial mediator of cognitive deficits (Chen et al., 2016; Zhang et al., 2020). Furthermore, the herbs that compose DZSM, including *E. breviscapus* (Vaniot) Hand.-Mazz., *P. ginseng* C.A. Mey., *O. japonicus* (Thunb.) Ker-Gawl., and *S. chinensis* (Turcz.) Baill., have shown multiple pharmacological activities in both experimental and clinical applications (Lin et al., 2019; Wan et al., 2021). Hence, these bioactive compounds and herbs may

FIGURE 9
Overview of the cognitive impairment-ameliorating mechanism of DZSM *via* CXCL12/CXCR4 regulation and microbial improvement.

form the basis for the beneficial role of DZSM in protecting against cognitive dysfunction.

To perform high-throughput characterization of the gene expression profiles at the tissue level, RNA-Seq was conducted on brain tissue. Transcriptomic analysis revealed that 196 of DEGs were reversed in the Aging-vs.-Nor and DZSM-vs.-Aging groups, indicating that the mechanism of DZSM in improving CI is polygenic, rather than involving a single gene. To identify key targets, for the combined treatment of cognitive deficits with DZSM, a PPI network was constructed. CXCR4 (degree = 19), a member of a family of highly conversed G protein-coupled receptors, was identified as a key target. CXCR4 has modulatory properties of neuron-glial interactions in the peripheral or central nervous system, such as in the neurons, astrocytes, and microglia (Li and Ransohoff, 2008). Recent studies indicated its vital role in neuromodulation, neuroprotection, and neuron-glial interaction communication, even improving neurological disorders such as infections, ischemia, cancer, and multiple unknown injuries (Hsiao et al., 2021). CXCL12, the ligand of CXCR4, regulates neuronal firing and neuron-glial interactive communication (Li et al., 2018). To date, increasing evidence has indicated that CXCL12 binding to CXCR4 triggers signal transduction pathways, showing multiple inflammatory-modulating activities,

including recruiting of perivascular macrophages in neuropathy (Mai et al., 2021), activating cells to secrete and release inflammatory cytokines (Dong et al., 2021), and promoting neuronal circuit formation (Peng et al., 2007). The results of quantitative real-time PCR and immunostaining shown that the expression of CXCL12 and CXCR4 was significantly suppressed in a dose-dependent manner after treatment with DZSM, indicating that DZSM exhibited neurocognitive function effects by modulating CXCR4 and CXCL12. Growing interest in the complex network of inflammatory mediators and immune system has enabled the identification of a growing number of pro-inflammatory molecules associated with CI and aging, such as IL-6, TNF-α, IL-18, and IL-1β (Cattaneo et al., 2017). Interestingly, chronic administration of DZSM was found to suppress neuroinflammation and alleviate the effects of aging and CI, as evidenced by the decreased levels of pro-inflammatory cytokines IL-6, TNF-α, IL-18, and IL-1β in aging mice after DZSM administration. These results suggest that DZSM could be a potential therapeutic agent for CI by suppressing neuroinflammation and modulating CXCR4 and CXCL12.

Multiple studies have shown that gut microbiota colonization is strongly associated with CI due to its adverse effects on metabolic disturbances or the progression of low-grade

inflammation leading to neurological dysfunction. Our findings are consistent with previous research indicating that a shift in the proportion of *Bacteroidia*, *Erysipelotrichia*, and *Deferribacteres* is closely related to increased inflammation (Jiao et al., 2018; Ren et al., 2021). Furthermore, our comprehensive analysis integrating transcriptomics and gut microbiota indicates that CXCL12 and CXCR4 modulate pro-inflammatory factors like IL-1β, IL-6, IL-18, and TNF-α and indirectly influence the composition or distribution of *Bacteroidia*, *Erysipelotrichia*, and *Deferribacteres* (Ng et al., 2011) (Figure 9). Our results suggest that the DZSM group had higher levels of *Deferribacteres* and lower levels of *Bacteroidia* and *Erysipelotrichia* compared to the Aging group. These changes were positively correlated with CXCR4, CXCL12, and inflammatory factors such as IL-1β, IL-6, IL-18, and TNF-α. We propose that the therapeutic benefits of DZSM for CI may be linked to its ability to regulate the inflammatory response and modulate the intestinal flora. Furthermore, our results suggest that the interaction between inflammatory cytokines and intestinal flora may contribute to the age-delaying effects of DZSM. Notably, *Bacteroidetes*, which constitute a significant proportion of the gut microbiota, have been shown to confer beneficial effects. Recent research indicates that the phylogenetic composition of human and mouse bacterial communities is similar at the phylum level, with *Bacteroidetes* and *Firmicutes* being the dominant phyla (Ley et al., 2006; Rawls et al., 2006). Coelho et al. (2018) have demonstrated that the gene content of *Bacteroidetes* and its response to diet are similar in both species. These findings suggest that the discovery of intestinal flora in mouse models may serve as a predictor of human microbiome results candidate biomarkers for early diagnosis (Kim et al., 2021). Our study also found a positive correlation between the proportion of *Bacteroidetes* and neurocognitive function, which is consistent with prior research (Shi et al., 2020; Xie et al., 2020). Meanwhile, in human microbiome studies, alterations in the proportion of *Bacteroidetes* have been linked to cognitive function. For instance, infants with higher *Bacteroidetes* strains at 1 year of age exhibit better cognitive performance at 2 years of age (Mariat et al., 2009), whereas cognitively impaired patients have lower abundances of *Bacteroidetes* strains in their gut microbiota (Carlson et al., 2018). *Erysipelotrichia,* a class of *Firmicutes* (Bhattacharjee et al., 2022), has also been found to be similar in both human and mouse flora (Coelho et al., 2018). Our study revealed a close association between the proportion of *Erysipelotrichia* and inflammatory cytokines, such as IL-6, IL-1, IL-1β, and IL-18 (Tang et al., 2022). *Erysipelotrichia* has been reported to produce high levels of anti-inflammatory short-chain fatty acids (Zhu et al., 2022) and is involved in immune regulation. However, it is also closely related to the production of inflammatory factors (Pindjakova et al., 2017), such as IL-6, IL-1 IL-1β, and IL-17, and has been found to be closely related to inflammatory diseases by Griffen et al. (2012). They performed the 16S pyrophosphate to detect the flora of healthy control and patients, further confirming that *Erysipelotrichia* was closely related to the prevalence of inflammatory diseases. *Deferribacteres*, on the other hand, is a pro-inflammatory bacterium that exhibits a protective effect by reducing low-grade chronic inflammation. It is closely associated with the pro-inflammatory cytokines IL-6, TNF-α, and IL-17A (Li

et al., 2019), which affect the cognitive function of the brain and the whole organism (Liang et al., 2018). In addition, alterations in the proportion of *Deferribacteres* have been also considered as potential microbiome markers for early diagnosis in clinical application. For instance, Kim et al. (2021) identified *Deferribacteres* as a candidate biomarker for early diagnosis of pancreatic cancer using microbial extracellular vesicles to detect microbiome compositional differences in blood samples from patients with pancreatic cancer and healthy controls. Although our study elucidated the mechanisms of DZSM in improving CIs, it remains unclear which of the main ingredients act individually or synergistically to create the observed effects. Therefore, further clinical and basic experiments are needed to investigate and identify the fundamental ingredients of DZSM in improving CIs.

Conclusion

The current study provides evidence that DZSM supplementation improved memory and cognitive function in a D-galactose-induced aging mouse model *via* comprehensively integrated transcriptomics and gut microbiota analyses. The underlying mechanism, whereby DZSM exerts its ameliorating effect on cognitive deficits appears to be mediated by the regulation of CXCL12/CXCR4, suppression of the expression of inflammatory cytokines, and adjustment of the intestinal flora composition, including *Bacteroidia*, *Erysipelotrichia*, and *Deferribacteres* species.

Data availability statement

The datasets presented in this study can be found in online repositories. The names of the repository/repositories and accession number(s) can be found below: NCBI BioProject (https://www.ncbi.nlm.nih.gov/bioproject/), PRJNA944587 and PRJNA946342.

Ethics statement

The animal study was reviewed and approved by Basic theories of Chinese Medical Sciences (Approval No. 2022B029).

Author contributions

Funding

Publisher's note

All claims expressed in this article are solely those of the authors and do not necessarily represent those of their affiliated organizations, or those of the publisher, the editors and the reviewers. Any product that may be evaluated in this article, or claim that may be made by its manufacturer, is not guaranteed or endorsed by the publisher.

Supplementary material

The Supplementary Material for this article can be found online at: https://www.frontiersin.org/articles/10.3389/fphar.2023.1175970/full#supplementary-material

SUPPLEMENTARY FIGURE S1
UPLC/MS analysis of DZMS. **(A)** Chromatogram of DZSM in positive ESI mode; **(B)** Chromatogram of DZSM in negative ESI mode.

References

Battle, C. E., Abdul-Rahim, A. H., Shenkin, S. D., Hewitt, J., and Quinn, T. J. (2021). Cholinesterase inhibitors for vascular dementia and other vascular cognitive impairments: A network meta-analysis. *Cochrane Database Syst. Rev.* 2 (2), CD013306. doi:10.1002/14651858.CD013306.pub2

Bhattacharjee, D., Flores, C., Woelfel-Monsivais, C., and Seekatz, A. M. (2022). Diversity and prevalence of Clostridium innocuum in the human gut microbiota. *mSphere.* 8. e0056922. doi:10.1128/msphere.00569-22

Budni, J., Pacheco, R., da Silva, S., Garcez, M. L., Mina, F., Bellettini-Santos, T., et al. (2016). Oral administration of d-galactose induces cognitive impairments and oxidative damage in rats. *Behav. Brain Res.* 302, 35–43. doi:10.1016/j.bbr.2015.12.041

Carlson, A. L., Xia, K., Azcarate-Peril, M. A., Goldman, B. D., Ahn, M., Styner, M. A., et al. (2018). Infant gut microbiome associated with cognitive development. *Biol. Psychiatry* 83 (2), 148–159. doi:10.1016/j.biopsych.2017.06.021

Cattaneo, A., Cattane, N., Galluzzi, S., Provasi, S., Lopizzo, N., Festari, C., et al. (2017). Association of brain amyloidosis with pro-inflammatory gut bacterial taxa and peripheral inflammation markers in cognitively impaired elderly. *Neurobiol. Aging* 49, 60–68. doi:10.1016/j.neurobiolaging.2016.08.019

Chen, X., Zhao, Z., Chen, Y., Gou, X., Zhou, Z., Zhong, G., et al. (2016). Mechanistic understanding of the effect of Dengzhan Shengmai capsule on the pharmacokinetics of clopidogrel in rats. *J. Ethnopharmacol.* 192, 362–369. doi:10.1016/j.jep.2016.07.066

Coelho, L. P., Kultima, J. R., Costea, P. I., Fournier, C., Pan, Y., Czarnecki-Maulden, G., et al. (2018). Similarity of the dog and human gut microbiomes in gene content and response to diet. *Microbiome* 6 (1), 72. doi:10.1186/s40168-018-0450-3

Dai, Y., Peng, L., Liu, Y., Xu, Y., and Qiao, J. (2021). Melatonin binds with high affinity and specificity to beta-amyloid: LC-MS provides insight into alzheimer's disease treatment. *FEBS Open Bio* 11 (10), 2800–2806. doi:10.1002/2211-5463.13279

Dong, J., Xia, R., Zhang, Z., and Xu, C. (2021). lncRNA MEG3 aggravated neuropathic pain and astrocyte overaction through mediating miR-130a-5p/CXCL12/CXCR4 axis. *Aging (Albany NY)* 13 (19), 23004–23019. doi:10.18632/aging.203592

Eshkoor, S. A., Hamid, T. A., Mun, C. Y., and Ng, C. K. (2015). Mild cognitive impairment and its management in older people. *Clin. Interv. Aging* 10, 687–693. doi:10.2147/CIA.S73922

Estebsari, F., Dastoorpoor, M., Khalifehkandi, Z. R., Nouri, A., Mostafaei, D., Hosseini, M., et al. (2020). The concept of successful aging: A review article. *Curr. Aging Sci.* 13 (1), 4–10. doi:10.2174/1874609812666191023130117

Go, J., Park, T. S., Han, G. H., Park, H. Y., Ryu, Y. K., Kim, Y. H., et al. (2018). Piperlongumine decreases cognitive impairment and improves hippocampal function in aged mice. *Int. J. Mol. Med.* 42 (4), 1875–1884. doi:10.3892/ijmm.2018.3782

Griffen, A. L., Beall, C. J., Campbell, J. H., Firestone, N. D., Kumar, P. S., Yang, Z. K., et al. (2012). Distinct and complex bacterial profiles in human periodontitis and health revealed by 16S pyrosequencing. *ISME J.* 6 (6), 1176–1185. doi:10.1038/ismej.2011.191

Hou, J. Y., Cao, G. Z., Tian, L. L., Zhou, R., Zhang, Y., Xu, H., et al. (2022). Integrated transcriptomics and metabolomics analysis reveals that C3 and C5 are vital targets of DuZhi Wan in protecting against cerebral ischemic injury. *Biomed. Pharmacother.* 155, 113703. doi:10.1016/j.biopha.2022.113703

Hou, J. Y., Wu, J. R., Xu, D., Chen, Y. B., Shang, D. D., Liu, S., et al. (2021). Integration of transcriptomics and system pharmacology to reveal the therapeutic mechanism underlying Qingfei Xiaoyan Wan to treat allergic asthma. *J. Ethnopharmacol.* 278, 114302. doi:10.1016/j.jep.2021.114302

Hou, Z., Qiu, R., Wei, Q., Liu, Y., Wang, M., Mei, T., et al. (2020). Electroacupuncture improves cognitive function in senescence-accelerated P8 (SAMP8) mice via the NLRP3/caspase-1 pathway. *Neural Plast.* 2020, 8853720. doi:10.1155/2020/8853720

Hsiao, C. C., Sankowski, R., Prinz, M., Smolders, J., Huitinga, I., and Hamann, J. (2021). GPCRomics of homeostatic and disease-associated human microglia. *Front. Immunol.* 12, 674189. doi:10.3389/fimmu.2021.674189

Isles, H. M., Herman, K. D., Robertson, A. L., Loynes, C. A., Prince, L. R., Elks, P. M., et al. (2019). The CXCL12/CXCR4 signaling Axis retains neutrophils at inflammatory sites in zebrafish. *Front. Immunol.* 10, 1784. doi:10.3389/fimmu.2019.01784

Jiao, N., Baker, S. S., Nugent, C. A., Tsompana, M., Cai, L., Wang, Y., et al. (2018). Gut microbiome may contribute to insulin resistance and systemic inflammation in obese rodents: A meta-analysis. *Physiol. Genomics* 50 (4), 244–254. doi:10.1152/physiolgenomics.00114.2017

Khan, M., Ullah, R., Rehman, S. U., Shah, S. A., Saeed, K., Muhammad, T., et al. (2019). 17β-Estradiol modulates SIRT1 and halts oxidative stress-mediated cognitive impairment in a male aging mouse model. *Cells* 8 (8), 928. doi:10.3390/cells8080928

Kim, J. R., Han, K., Han, Y., Kang, N., Shin, T. S., Park, H. J., et al. (2021). Microbiome markers of pancreatic cancer based on bacteria-derived extracellular vesicles acquired from blood samples: A retrospective propensity score matching analysis. *Biol. (Basel)* 10 (3), 219. doi:10.3390/biology10030219

Ley, R. E., Turnbaugh, P. J., Klein, S., and Gordon, J. I. (2006). Microbial ecology: Human gut microbes associated with obesity. *Nature* 444 (7122), 1022–1023. doi:10.1038/4441022a

Li, H., Hao, L., Li, Y., and Wang, R. (2018). Reducing CXCR4 resulted in impairing proliferation and promoting aging. *J. Nutr. Health Aging* 22 (7), 785–789. doi:10.1007/s12603-018-1013-9

Li, H., Zheng, L., Chen, C., Liu, X., and Zhang, W. (2019). Brain senescence caused by elevated levels of reactive metabolite methylglyoxal on D-galactose-induced aging mice. *Front. Neurosci.* 13, 1004. doi:10.3389/fnins.2019.01004

Li, L., Zhang, H., Chen, B., Xia, B., Zhu, R., Liu, Y., et al. (2022). BaZiBuShen alleviates cognitive deficits and regulates Sirt6/NRF2/HO-1 and Sirt6/P53-PGC-1α-TERT signaling pathways in aging mice. *J. Ethnopharmacol.* 282, 114653. doi:10.1016/j.jep.2021.114653

Li, M., and Ransohoff, R. M. (2008). Multiple roles of chemokine CXCL12 in the central nervous system: A migration from immunology to neurobiology. *Prog. Neurobiol.* 84 (2), 116–131. doi:10.1016/j.pneurobio.2007.11.003

Liang, S., Wu, X., and Jin, F. (2018). Gut-brain psychology: Rethinking psychology from the microbiota-gut-brain Axis. *Front. Integr. Neurosci.* 12, 33. doi:10.3389/fnint.2018.00033

Lin, T. L., Lu, C. C., Lai, W. F., Wu, T. S., Lu, J. J., Chen, Y. M., et al. (2021). Role of gut microbiota in identification of novel TCM-derived active metabolites. *Protein Cell* 12 (5), 394–410. doi:10.1007/s13238-020-00784-w

Lin, Y., Ren, N., Li, S., Chen, M., and Pu, P. (2019). Novel anti-obesity effect of scutellarein and potential underlying mechanism of actions. *Biomed. Pharmacother.* 117, 109042. doi:10.1016/j.biopha.2019.109042

Mai, C. L., Tan, Z., Xu, Y. N., Zhang, J. J., Huang, Z. H., Wang, D., et al. (2021). CXCL12-mediated monocyte transmigration into brain perivascular space leads to neuroinflammation and memory deficit in neuropathic pain. *Theranostics* 11 (3), 1059–1078. doi:10.7150/thno.44364

Mariat, D., Firmesse, O., Levenez, F., Guimaraes, V., Sokol, H., Dore, J., et al. (2009). The Firmicutes/Bacteroidetes ratio of the human microbiota changes with age. *BMC Microbiol.* 9, 123. doi:10.1186/1471-2180-9-123

Mu, X., Xu, X., Guo, X., Yang, P., Du, J., Mi, N., et al. (2019). Identification and characterization of chemical constituents in Dengzhan Shengmai Capsule and their metabolites in rat plasma by ultra-performance liquid chromatography coupled with quadrupole time-of-flight mass spectrometry. *J. Chromatogr. B Anal. Technol. Biomed. Life Sci.* 1108, 54–64. doi:10.1016/j.jchromb.2019.01.010

Ng, S. C., Benjamin, J. L., McCarthy, N. E., Hedin, C. R., Koutsoumpas, A., Plamondon, S., et al. (2011). Relationship between human intestinal dendritic cells, gut microbiota, and disease activity in Crohn's disease. *Inflamm. Bowel Dis.* 17 (10), 2027–2037. doi:10.1002/ibd.21590

O'Brien, J. T., Holmes, C., Jones, M., Jones, R., Livingston, G., McKeith, I., et al. (2017). Clinical practice with anti-dementia drugs: A revised (third) consensus statement from the British association for psychopharmacology. *J. Psychopharmacol.* 31 (2), 147–168. doi:10.1177/0269881116680924

Pei, H., Ma, L., Cao, Y., Wang, F., Li, Z., Liu, N., et al. (2020). Traditional Chinese medicine for alzheimer's disease and other cognitive impairment: A review. *Am. J. Chin. Med.* 48 (3), 487–511. doi:10.1142/S0192415X20500251

Peng, H., Kolb, R., Kennedy, J. E., and Zheng, J. (2007). Differential expression of CXCL12 and CXCR4 during human fetal neural progenitor cell differentiation. *J. Neuroimmune Pharmacol.* 2 (3), 251–258. doi:10.1007/s11481-007-9081-3

Pindjakova, J., Sartini, C., Lo Re, O., Rappa, F., Coupe, B., Lelouvier, B., et al. (2017). Gut dysbiosis and adaptive immune response in diet-induced obesity vs. Systemic inflammation. *Front. Microbiol.* 8, 1157. doi:10.3389/fmicb.2017.01157

Ratan, Z. A., Youn, S. H., Kwak, Y. S., Han, C. K., Haidere, M. F., Kim, J. K., et al. (2021). Adaptogenic effects of Panax ginseng on modulation of immune functions. *J. Ginseng Res.* 45 (1), 32–40. doi:10.1016/j.jgr.2020.09.004

Rawls, J. F., Mahowald, M. A., Ley, R. E., and Gordon, J. I. (2006). Reciprocal gut microbiota transplants from zebrafish and mice to germ-free recipients reveal host habitat selection. *Cell* 127 (2), 423–433. doi:10.1016/j.cell.2006.08.043

Ren, S. M., Zhang, Q. Z., Chen, M. L., Jiang, M., Zhou, Y., Xu, X. J., et al. (2021). Anti-NAFLD effect of defatted walnut powder extract in high fat diet-induced C57BL/6 mice by modulating the gut microbiota. *J. Ethnopharmacol.* 270, 113814. doi:10.1016/j.jep.2021.113814

Ricker, L. J., Kijlstra, A., Kessels, A. G., de Jager, W., Liem, A. T., Hendrikse, F., et al. (2011). Interleukin and growth factor levels in subretinal fluid in rhegmatogenous retinal detachment: A case-control study. *PLoS One* 6 (4), e19141. doi:10.1371/journal.pone.0019141

Sanfilippo, C., Castrogiovanni, P., Imbesi, R., Nunnari, G., and Di Rosa, M. (2020). Postsynaptic damage and microglial activation in AD patients could be linked CXCR4/CXCL12 expression levels. *Brain Res.* 1749, 147127. doi:10.1016/j.brainres.2020.147127

Sheng, N., Zheng, H., Xiao, Y., Wang, Z., Li, M., and Zhang, J. (2017). Chiral separation and chemical profile of Dengzhan Shengmai by integrating comprehensive with multiple heart-cutting two-dimensional liquid chromatography coupled with quadrupole time-of-flight mass spectrometry. *J. Chromatogr. A* 1517, 97–107. doi:10.1016/j.chroma.2017.08.037

Shi, H., Yu, Y., Lin, D., Zheng, P., Zhang, P., Hu, M., et al. (2020). β-glucan attenuates cognitive impairment via the gut-brain axis in diet-induced obese mice. *Microbiome* 8 (1), 143. doi:10.1186/s40168-020-00920-y

Shi, L., Bi, Q., Li, W., Qin, L., and Yang, P. (2016). CXCL12 impairs the acquisition and extinction of auditory fear conditioning in rats via crosstalk with GABAergic system. *Pharmacol. Biochem. Behav.* 148, 21–27. doi:10.1016/j.pbb.2016.05.008

Slanina, J., Taborska, E., and Lojkova, L. (1997). Lignans in the seeds and fruits of Schisandra chinensis cultured in Europe. *Planta Med.* 63 (3), 277–280. doi:10.1055/s-2006-957676

Song, Q., Fang, H., and Ye, X. (2018). Clinical analysis of Dengzhan Shengmai capsule in the treatment of cognitive dysfunction in post-stroke patients. *Zhejiang Pract. Med.* 23, 82–84.

Sun, K., Yang, P., Zhao, R., Bai, Y., and Guo, Z. (2018). Matrine attenuates D-galactose-induced aging-related behavior in mice via inhibition of cellular senescence and oxidative stress. *Oxid. Med. Cell Longev.* 2018, 7108604. doi:10.1155/2018/7108604

Tang, Y., Pu, Q., Zhao, Q., Zhou, Y., Jiang, X., and Han, T. (2022). Effects of fucoidan isolated from laminaria japonica on immune response and gut microbiota in cyclophosphamide-treated mice. *Front. Immunol.* 13, 916618. doi:10.3389/fimmu.2022.916618

Wan, Y., Wang, J., Xu, J. F., Tang, F., Chen, L., Tan, Y. Z., et al. (2021). Panax ginseng and its ginsenosides: Potential candidates for the prevention and treatment of chemotherapy-induced side effects. *J. Ginseng Res.* 45 (6), 617–630. doi:10.1016/j.jgr.2021.03.001

Wang, X. S., and Huang, H. (2018). Study of molecular mechanisms of learning and memory impairment in neonatal rats post intrauterine distress via the pathway of Tau protein hyperphosphorylation. *Eur. Rev. Med. Pharmacol. Sci.* 22 (9), 2787–2800. doi:10.26355/eurrev_201805_14978

Xie, Z., Lu, H., Yang, S., Zeng, Y., Li, W., Wang, L., et al. (2020). Salidroside attenuates cognitive dysfunction in senescence-accelerated mouse prone 8 (SAMP8) mice and modulates inflammation of the gut-brain Axis. *Front. Pharmacol.* 11, 568423. doi:10.3389/fphar.2020.568423

Yang, M., Tong, L., Wang, S., Liu, N., Zhao, F., Sun, Y., et al. (2022). Gut microbiota and transcriptomics reveal the effect of human norovirus bioaccumulation on oysters (*Crassostrea gigas*). *Microbiol. Spectr.* 10 (4), e0016122. doi:10.1128/spectrum.00161-22

Zhang, S., Zhang, J., Wei, D., An, H., Liu, W., Lai, Y., et al. (2020). Dengzhan Shengmai capsules and their active component scutellarin prevent cognitive decline in APP/PS1 mice by accelerating Aβ aggregation and reducing oligomers formation. *Biomed. Pharmacother.* 121, 109682. doi:10.1016/j.biopha.2019.109682

Zhu, T., Wang, Z., He, J., Zhang, X., Zhu, C., Zhang, S., et al. (2022). D-galactose protects the intestine from ionizing radiation-induced injury by altering the gut microbiome. *J. Radiat. Res.* 63 (6), 805–816. doi:10.1093/jrr/rrac059

Glossary

The following abbreviations are used in this document:

AD Alzheimer's Disease

ANOVA Analysis of variance

BP Biological process

BSA Bovine Serum Albumin

CC Cellular component

CI Cognitive impairment

CXCL12 CXC chemokine ligand 12

CXCR4 Chemokine CXC motif receptor 4

DEG Differentially expressed genes

DZSM Dengzhan Shengmai

ELISA Enzyme-linked immunosorbent assay

ESI electrospray ionization

GO Gene Ontology

H&E Hematoxylin and eosin

HRP Horseradish peroxidase

IL-1β Interleukin-1β

IL-6 Interleukin-6

IL-18 Interleukin-18

KEGG Kyoto Encyclopedia of Genes and Genomes

LDA Linear discriminant analysis

MF Molecular function

MMSE Mini-mental State Examination

MoCA Montreal Cognitive Assessment

MWM Morris water maze

OFT Open field task

OTU Operational taxonomic units

PBS Phosphate-buffered saline

PCoA principal coordinates analysis

PCR Polymerase chain reaction

PPI Protein–protein interaction

RDA redundancy analysis

RNA Ribonucleic acid

SCFAs short-chain fatty acids

TCM Traditional Chinese medicine

TIC total ion chromatogram

TNF-α Tumor necrosis factor-α

UPGMA Unweighted pair group method with arithmetic.